Electromagnetic Coupling Reduction Techniques

Eighth Quarterly Report

15 August - 14 November 1967

By

J.A.M. Lyon, C.J. Digenis, W.W. Parker
A.G. Cha and M.A.H. Ibrahim.

December 1967

Contract No. AF 33(615)-3371
Project 4357, Task 435709

Prepared for

Air Force Avionics Laboratory
United States Air Force, AFSC
Wright-Patterson AFB, Ohio 45433

FOREWORD

This report was prepared by The University of Michigan, Ann Arbor, Michigan, under the direction of Professor Ralph E. Hiatt and Professor John A.M. Lyon and on Air Force Contract AF 33(615)-3371 under Task No. 435709 of Project 4357 (U) "Electromagnetic Coupling Reduction Techniques". The work was administered under the direction of the Air Force Avionics Laboratory, Electronic Warfare Division, Research and Technology Division, Wright-Patterson Air Force Base Ohio. The Task Engineer was Mr. Olin E. Horton, the Project Engineer Mr. Herbert Bartman.

This report covers the period 15 August through 14 November 1967.

ABSTRACT

In this report further studies on some previously described decoupling methods are presented. Slot decoupling has been examined at a lower range of frequencies (S-band). The behavior of corrugations at three times the design frequency has also been studied. The use of circumferential corrugations as a decoupling means was extended to circular Archimedean spiral antennas. Studies initiated in this report period include the coupling of two X-band slot antennas covered by a dielectric sheet. It has been found that under some conditions the presence of the sheet results in decoupling, whereas in other cases increased coupling results.

TABLE OF CONTENTS

	Page
FOREWORD	iii
ABSTRACT	iv
LIST OF FIGURES	vi
I INTRODUCTION	1
II PROGRESS IN DECOUPLING METHODS	3
2.1 Corrugations	3
2.1.1 Design Considerations	3
2.1.2 Slot Decoupling	6
2.1.3 Spiral Decoupling	13
2.2 Coupling Under Dielectric Layers	20
2.3 Theoretical Analysis of Slots in a Ground Plane	24
2.4 Current Distribution on a Rectangular Spiral Antenna	25
III CONCLUSIONS	30
IV FUTURE EFFORT	31
ACKNOWLEDGEMENT	31
REFERENCES	31
DD FORM 1473	
DISTRIBUTUION LIST	

LIST OF FIGURES

Figure No.	Captions	Page
2-1	Slot Antenna and Corrugations.	5
2-2	E - And H-Plane Coupling vs Frequency for Two Slots Spaced 22.8 cm in a 12' Aluminum Ground Plane.	7
2-3	Radiation Patterns for an S-Band Slot in a Metal Disc of 33.3 cm Diameter. (——) Flat Disc; (—●—) with Corrugations.	8
2-4	Maximum Gain vs. Frequency for an S-Band Slot in a Metal Disc of 33.3 dm Diameter.	10
2-5	E-Plane Coupling vs Frequency for Two Slots Spaced 22.8 cm. Parameter Indicates the Number of Uncovered Trenches.	11
2-6	E-Plane Coupling vs Frequency for Two X-Band Slots Spaced 22.8 cm.	12
2-7	Relative Positions of Circular Spirals (Feeds).	15
2-8	Coupling vs Frequency for Two Archimedean Spirals Spaced 22.8 cm.	16
2-9	Radiation Patterns of an Archimedean Spiral in a 2 ft. by 3 ft. Metal Ground Plane for Two Normal Linear Polarizations. (——) Flat Plane; (—●—) with Corrugations.	18
2-10	Slot Coupling with 40 Inch by 20 inch by 1/8 inch Polystyrene Sheet.	21
2-11	Slot Coupling with 40 inch by 20 inch by 1/4 inch Polystyrene Sheet.	22
2-12	Slot Coupling with 40 inch by 20 inch by 1/2 inch Polystyrene Sheet.	23

List of Figures (cont'd)

Figure No.	Captions	Page
2-13	Amplitude and Phase of the Current Excited on one Arm of the Rectangular Spiral. f = 400MHz (x) Amplitude (△) Phase.	26
2-14	Measurement of the Transverse Component of H-Field along an Axis X-X on the Spiral Surface.	28
2-15	Amplitude and Phase of H Field With and Without the Spiral Scatterer in Place. (△) With Spiral (X) Without Spiral	29

I

INTRODUCTION

This investigation can logically be separated into three technical areas. The technical areas are decoupling achieved by corrugations; decoupling or coupling associated with a dielectric slab over rectangular slot antennas; advanced analysis of coupling between slots to be applicable to the nearfield region.

In Section 2.1 of this report, a detailed description has been given of a newly designed arrangement of circumferential corrugations. These corrugations have been designed to be operable in the S-band of frequencies. The design frequency has been near the lower end of this band. Design procedures and design parameters are given. After this new set of corrugations was fabricated it was used to ascertain the decoupling achieved in the case of two slot radiators. The maximum decoupling achieved was approximately 14 db. In the body of the report, information is given on the bandwidth covered by this means of decoupling. Later, the same set of corrugations was utilized at three-times the design frequency. It was found that this set of corrugations produced a maximum decoupling of approximately 15 db in the X-band of frequencies.

The new set of S-band corrugations was then applied to the case of two Archimedean circular spirals. It was found that the one set of corrugations around one of the spirals produced a maximum reduction in coupling of 6 db. This was within the design frequency range of 2.0 to 4.0 GHz. The effect of a set of corrugations surrounding an Archimedean spiral is also shown in radiation patterns included in this report.

The influence of dielectric cover plates over two rectangular slot antennas has been studied experimentally. Details of these studies are shown in Section 2.2. Several slabs of material were utilized including wood and polystyrene.

Also, various size sheets and thicknesses were utilized. The influence of scatter from the boundaries of the sheet is also discussed.

Still another effort covered in the report is that of the improved analysis of two rectangular slot antennas. This analysis is aimed at being sufficiently precise so as to predict the nearfield coupling situation for the parallel alignment of the two slots. So far only initial formulation has been made. No experiments have been performed but some have been planned.

II

PROGRESS IN DECOUPLING METHODS

2.1 Corrugations

2.1.1 Design Considerations

A new set of circumferential corrugations has been designed and fabricated for use with antennas operating at S-band frequencies. The design formula is obtained as follows. A two-dimensional periodic structure is considered. The trenches are assumed narrow enough so that only a TEM-mode propagates in them. If d, and w are the trench depth and width respectively, s the center-to-center spacing of adjacent trenches and η the free space charecteristic impedance, the surface impedance of the corrugated structure is:

$$Z_s = \begin{cases} j\eta \tan kd & \text{(trench aperture, } w) \\ 0 & \text{(wall separating trenches, } s-w) \end{cases} \quad (2.1)$$

A TM-mode is assumed above the corrugations. By using Floquet's theorem for periodic structures and considering an infinite number of space-harmonics above the surface in order to satisfy the boundary condition as stated in (2.1) an equation is derived from which the phase constants of the space harmonics can be determined. At the frequency where the cut-off of the first pass-band occurs this equation is simplified to the following form (Watkins, 1958)

$$\frac{1}{kd \tan kd} = \frac{2s}{\pi^2 d} \sum_n \frac{1}{(1+2n)} \cdot \frac{\left[\sin (1+2n) \frac{\pi w}{2s}\right]}{(1+2n)} \quad (2.2)$$

$$n = o, \pm 1, \pm 2, \ldots$$

This equation can be solved by graphical methods or by trial and error. There are three parameters d, w, and s which have to be chosen to determine the propagation parameter k from which the frequency will be obtained. An examination of (2.2) shows that the most critical parameter is d. As a starting point for a trial and error solution, the value $d=\frac{\lambda}{4}$ may be used,

(λ = wavelength). Considering (2.1) and using the concept of "average surface impedance" one obtains:

$$Z_{s,\ ave} = j\eta \frac{w}{s} \tan kd \qquad (2.3)$$

It has been shown (Lyon et al, May 1966) that a greater Z_s produces greater decoupling. Because of this in (2.3) it is desirable to make $\frac{w}{s}$ as big as possible (the upper limit being 1) which means making the wall thickness (s-w) as small as possible. Here a limit is imposed by consideration of the metal and manufacturing method used.

Finally regarding w there are two reasons for making it as large as possible. First, for the same reasons that one wants to make (s-w) as small as possible. Second, because of consideration of the ω-β diagram for this structure (Watkins, 1958) which shows that the larger s/d the more the cut-off deviates from the value $kd = \frac{\pi}{2}$ causing the stop band to increase which is desirable in broadband applications of the method. On the other hand there is an upper limit imposed by the conditions under which (2.2) was derived, namely that the trenches are narrow enough so only a TEM-mode propagates inside. In order to obtain reasonably accurate results from (2.2) one would have to limit w to $\lambda/10$ although values of $w \sim \lambda/3$ have been used as described later with good agreement with (2.2).

In view of the above considerations, the dimensions of the corrugations for S-band were chosen as follows:

$$d = 2.41 \text{ cm} \qquad w = 0.81 \text{ cm} \qquad s = 0.89 \text{ cm}.$$

These corrugations extend radially for 11.46 cm (1.3λ at 3.4 GHz) (Fig. 2-1). The cut-off frequency for the first pass band is found from (2-1) to be 2.75 GHz and for the second pass band 8.31 GHz. Thus the corrugations should be effective in reducing coupling at both S- and X-bands.

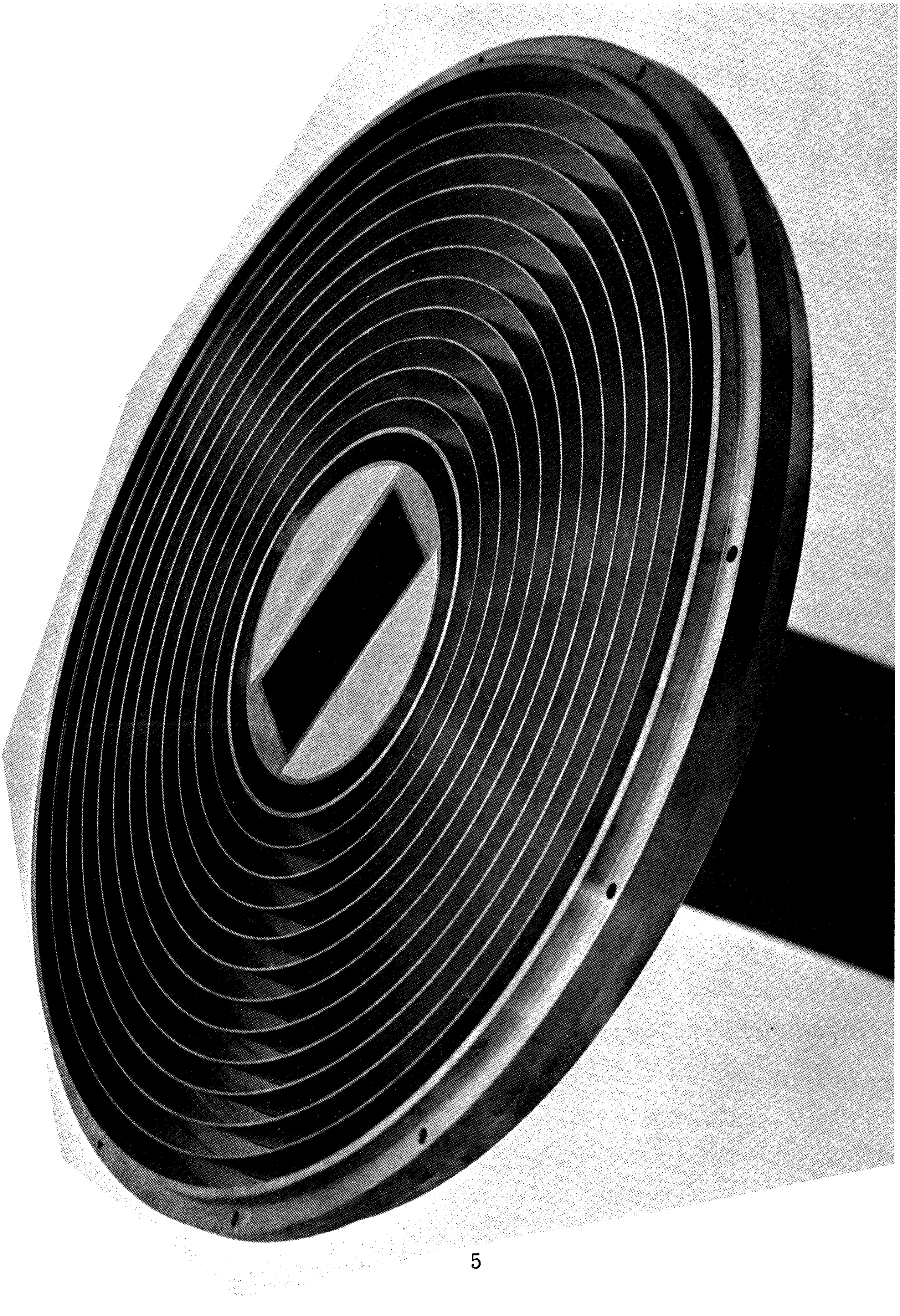

FIG. 2-1: SLOT ANTENNA AND CORRUGATIONS.

2.1.2 Slot Decoupling

When these corrugations were placed around an S-band slot it was found that the E-plane coupling to an adjacent slot was reduced from a maximum value of -27 db to -41 db over almost the entire S-band (see Fig. 2-2). The center-to-center spacing of the two slots was 2.5λ in the middle of the frequency range considered (3.3 GHz). The experiment also indicates the stop band starts at 2.81 GHz which is 2.1 percent off the calculated value. When the slots are oriented for weak coupling (H-planes colinear) the radiation pattern of each slot exhibits a null in the direction of the other slot and therefore the corrugations cannot be as effective. However this is not a serious problem since the H-plane coupling level is much lower than the E-plane coupling, In this case the maximum H-plane coupling was reduced from -49 db to -52 db when the corrugations were added. In the case of H-plane coupling the stop band starts at 2.73 GHz which is within the limits of measurement error from the calculated value. This agreement with the theoretical result is remarkable; it is even more so since the actual geometry deviates from that assumed to derive (2.2) on two counts: a) The structure is not periodic since it extends for only one wavelength rather than continuing to infinity and b) instead of parallel wall corrugations one has circumferential corrugations which, strictly speaking, is not a two-dimensional problem.

The action of the corrugations has been qualitatively explained as trapping the power carried by a surface wave along the ground plane and radiating it in the broadside direction. This means that the sidelobe decrease should be accompanied by an antenna gain increase. This was observed experimentally by mounting the slot on a small metal disc (diameter 33.3 cm) and recording the radiation patterns in the two main planes, (see Fig. 2-3). A plain and a corrugated disc were interchanged and the two curves superimposed for comparison. At

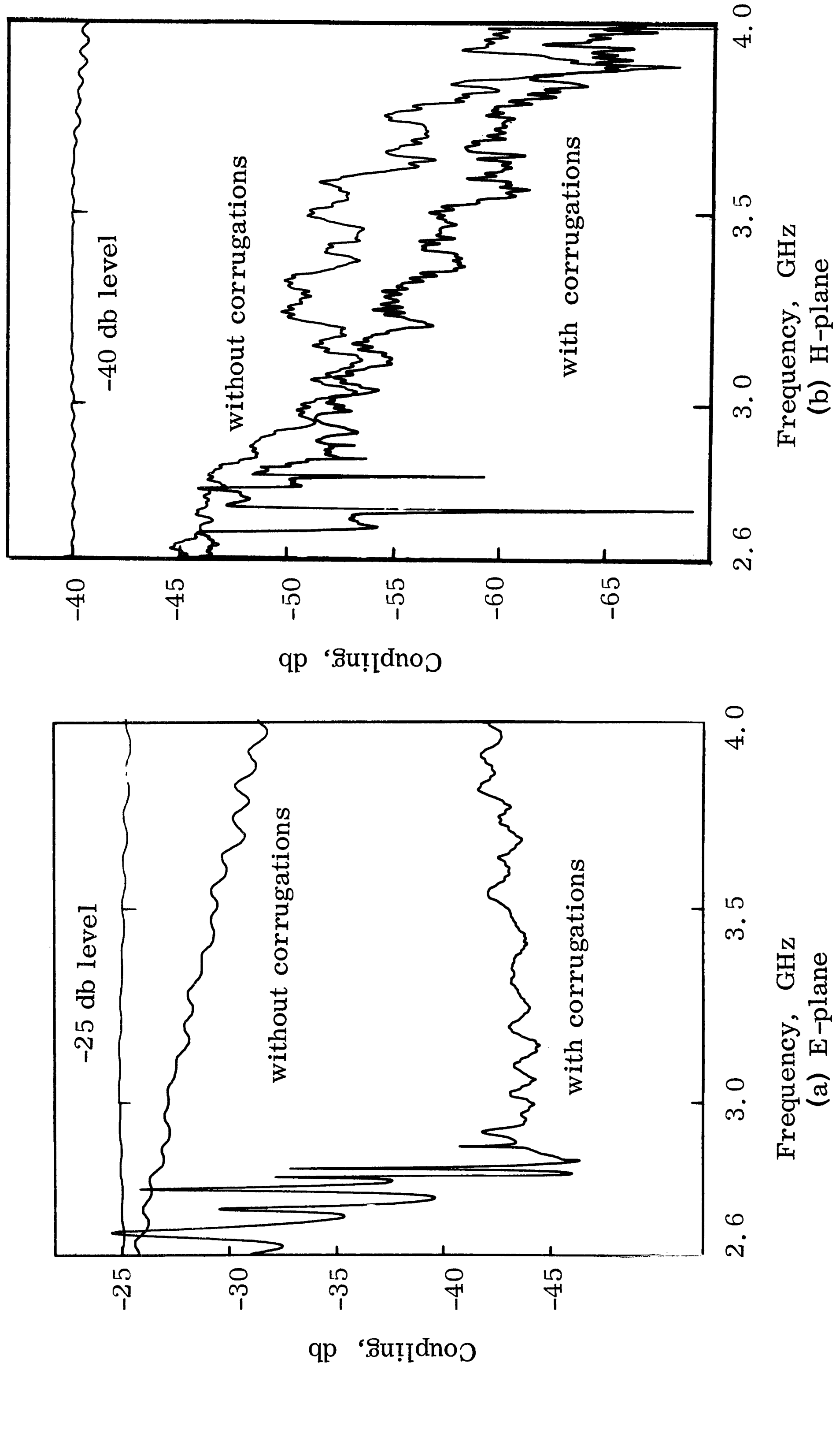

FIG. 2-2: E- AND H-PLANE COUPLING VS FREQUENCY FOR TWO SLOTS SPACED 22.8 CM IN A 12' BY 12' ALUMINUM GROUND PLANE.

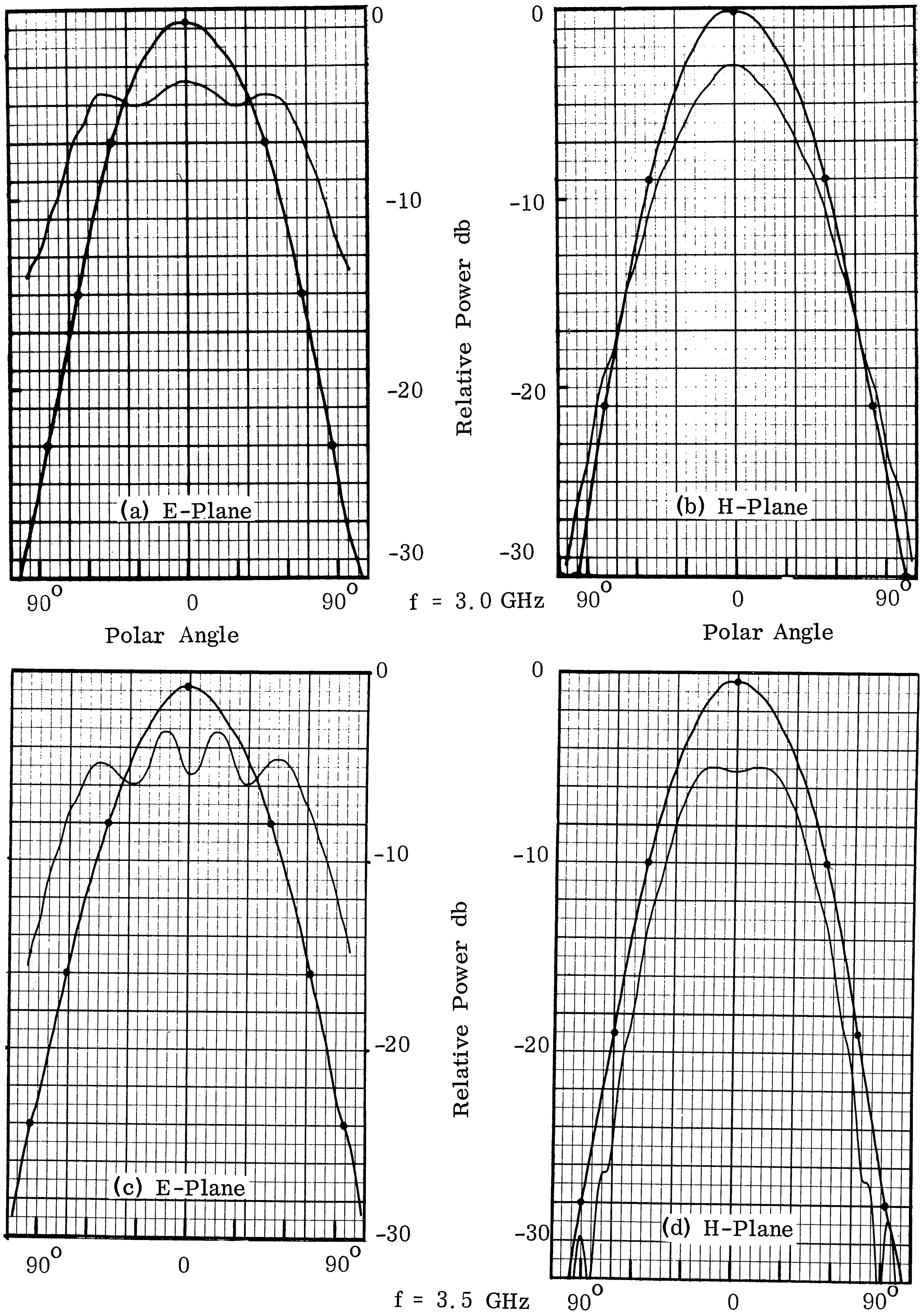

FIG. 2-3: RADIATION PATTERNS FOR AN S-BAND SLOT IN A METAL DISC OF 33.3 CM DIAMETER. (—) Flat Disc; (—•—)Disc with Corrugations.

3.0 GHz the corrugations cause an E-plane sidelobe reduction of 12 db accompanied by a 3 db gain increase. By orienting the slot for maximum gain and sweeping the frequency (Fig. 2-4) it was demonstrated that the gain increase varies between 1.5 db to 5.0 db over the frequencies of S-band.

It has been thought of interest to investigate the effect on decoupling of the trenches individually. For this purpose the area of the ground surface represented by the corrugations was covered by aluminum foil and the coupling between the two slots measured by sweeping the frequency. Then the innermost trench was uncovered and the coupling measured again. The uncovering of subsequent trenches continued until all were active. The results are shown in Fig. 2-5. In this figure the parameter indicates the number of uncovered trenches. The lowest curve in Fig. 2-5 is identical with that of Fig. 2-2(a). By examining Fig. 2-5 it is clearly seen that incremental steps of decoupling do not show a tendency to shrink to zero very rapidly, which indicates that additional decoupling is possible by extending the corrugations further.

Another experiment was carried out to test the effect of the corrugations at the second stop band. Regarding the corrugations designed for S-band the second stop band occurs at nearly the third harmonic frequencies of the first stop band which in this case would be X-band.

An X-band slot surrounded by a small flat disc was placed at the center of the S-band corrugations. Then the coupling to a second slot on the same ground plane was measured when the corrugations S were covered by aluminum foil and when they were uncovered. The results are shown in Fig. 2-6 (second and fourth curves from the top, respectively). It is seen that the stop band starts at 8.34 GHz which is again within measurement error from the theoretically computed value of 8.31 GHz. Then the disc between the slot and corrugations S was replaced by another set of corrugations (designated R-1, d = 0.85 cm) which

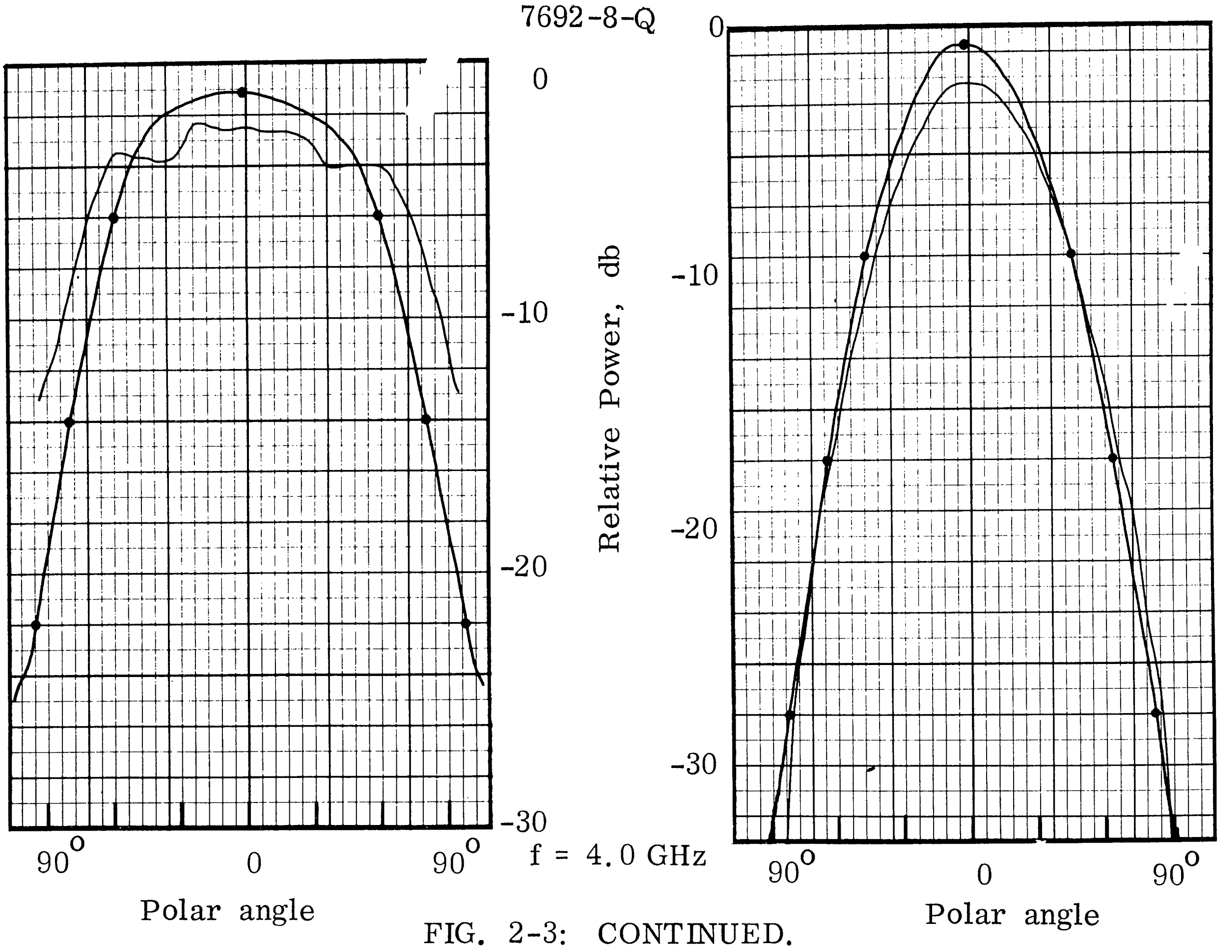

FIG. 2-3: CONTINUED.

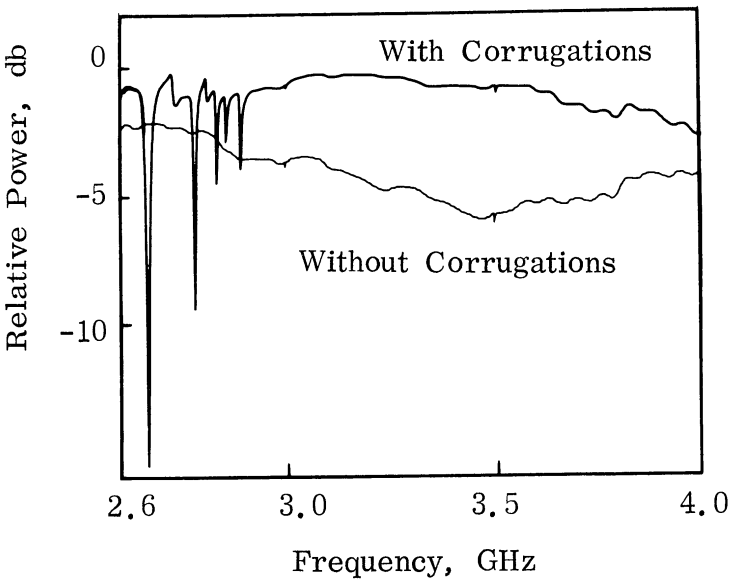

FIG. 2-4: MAXIMUM GAIN VS. FREQUENCY FOR AN S-BAND SLOT IN A METAL DISC OF 33.3 CM DIAMETER.

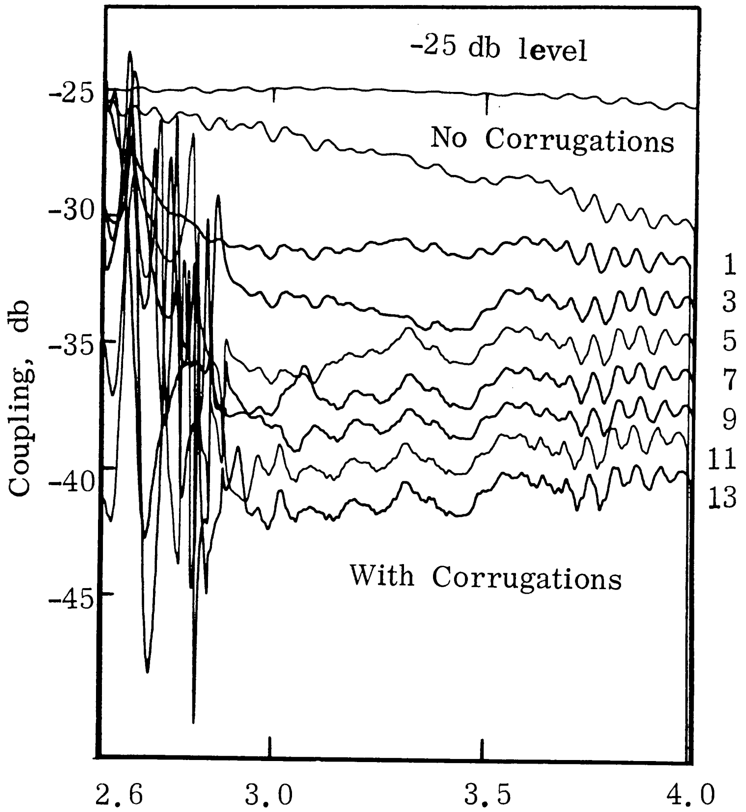

FIG. 2-5: E-PLANE COUPLING VS FREQUENCY FOR TWO SLOTS SPACED 22.8 CM. Parameter Indicates the Number of Uncovered Trenches.

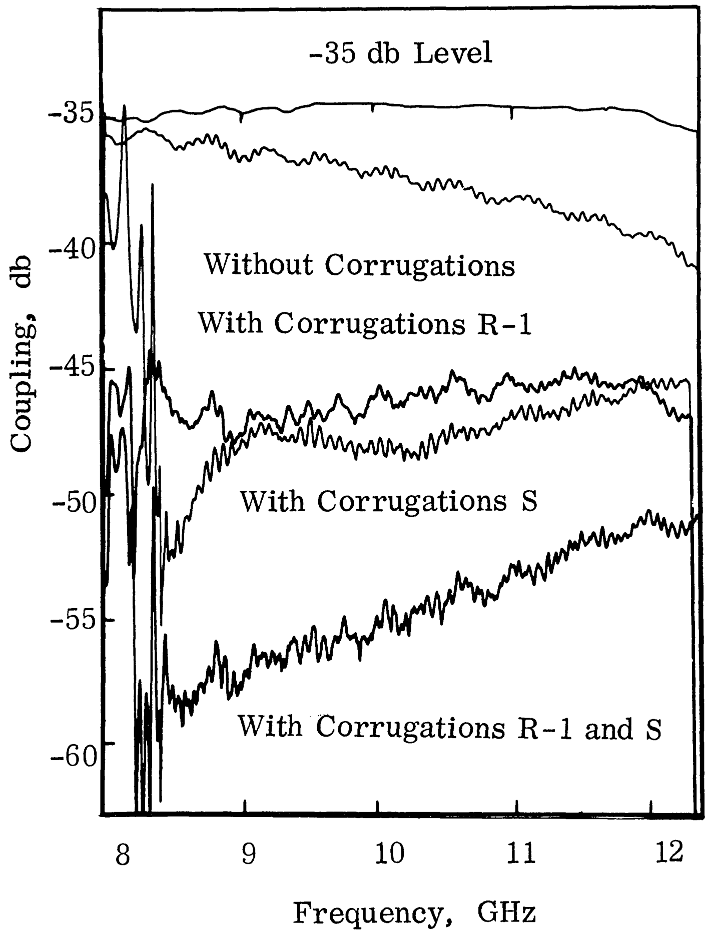

FIG. 2-6: E-PLANE COUPLING VS FREQUENCY FOR TWO X-BAND SLOTS SPACED 22.8 CM.

has been designed for X-band. Again two measurements were made with the corrugations S covered and uncovered. The results are shown in Fig. 2-6 (third and fifth curves from the top, respectively). The maximum E-plane coupling over almost all of the X-band has been reduced from -35.5 db to -50.5 db.

In conclusion it is seen that the corrugations are inherently effective also in reducing coupling at the third harmonic frequencies of the original design frequency range. This is an important feature because of the third harmonic content in the output at microwave oscillators in particular and in the radiation of various antennas in general. Due to this phenomenon several interference problems have been reported between antennas operating at different frequencies.

2.1.3 Spiral Decoupling

When a spiral operates in a pure axial (on first order) mode there is a null along the ground plane and the coupling to another spiral in the same ground plane should be zero. In actual operation, however, reflections from the ends of the spiral elements may occur giving rise to a standing wave along the spiral arms. Also small in-phase currents at the feed excite additional modes, of order zero, two, etc. The zero order mode in particular will cause a considerable amount of radiation along the ground plane. These feed and termination defects are considered to be primarily responsible for the coupling between two spirals. Therefore this is a case of weak coupling comparable to the H-plane coupling of slots.

Two similar Archimedean spirals made by Aero Geo-Astro Corporation (Model AGA-100-3-2) for the frequency range 2 GHz to 4 GHz were used for the measurement of coupling. The two spirals were mounted in a large (12 ft. by 12 ft.) ground plane at a center-to-center spacing of 22.8 cm (2.5λ at 3.3 GHz). The coupling measurements were made by a swept frequency technique. Due to this no matching devices were used between the transmission line and the antennas. A spot check, however, indicated that the use of matching devices results in no more than 1 db difference in the coupling level. However the defects of the feeds to the spirals are emphasized in swept frequency methods.

For the coupling measurements the two spirals were positioned in three different ways as shown in Fig. 2-7. In this figure the positions of the spirals are determined from the relative orientation of the feed terminals. One of the spiral antennas was surrounded by circumferential corrugations and then the coupling was measured with the corrugations covered and then uncovered. The two curves obtained for every orientation of the feed terminals are shown in Figure 2-8a through c. For any given frequency the coupling depends upon the relative orientation of the two spirals. However, the swept frequency coupling patterns taken for different orientations exhibit the same general characteristics except that the peaks and troughs occur at different frequencies. The corrugations accomplished a moderate coupling reduction of 6 db in the frequency range 2.8 to 4.0 GHz.

The effects of the corrugations on the spiral radiation pattern at different frequencies are shown in Fig. 2-9. These patterns were obtained by illuminating the spiral with a linearly polarized standard gain horn. The polarization was chosen so that the E-field vector would be perpendicular to the ground plane at $\theta = 90^{\circ}$. The patterns are shown for two different orientations of the spiral; one where the (imaginary) line determined by the two feed points is parallel to the E-field and another where it is perpendicular. A sidelobe decrease of the order of 6 to 11 db is observed, accompanied by a gain increase. The gain increase due to the corrugations varies from 1 db at the low end of the frequency range to zero db at the high end.

The change in VSWR is summarized in the following table.

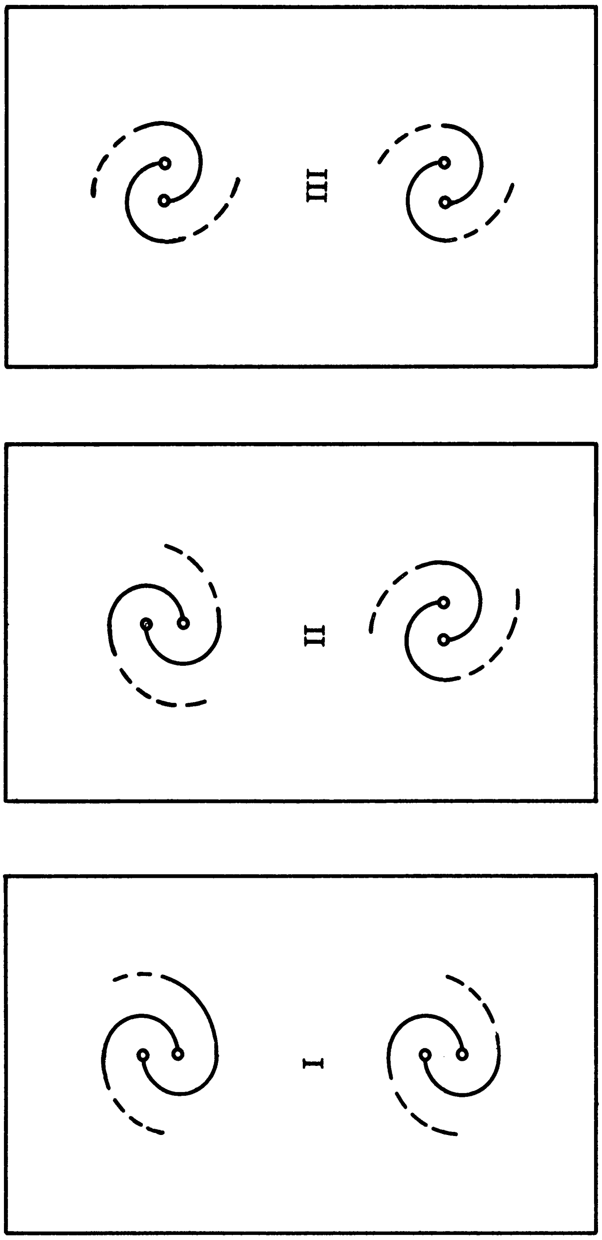

FIG. 2-7: RELATIVE POSITIONS OF CIRCULAR SPIRALS (FEEDS).

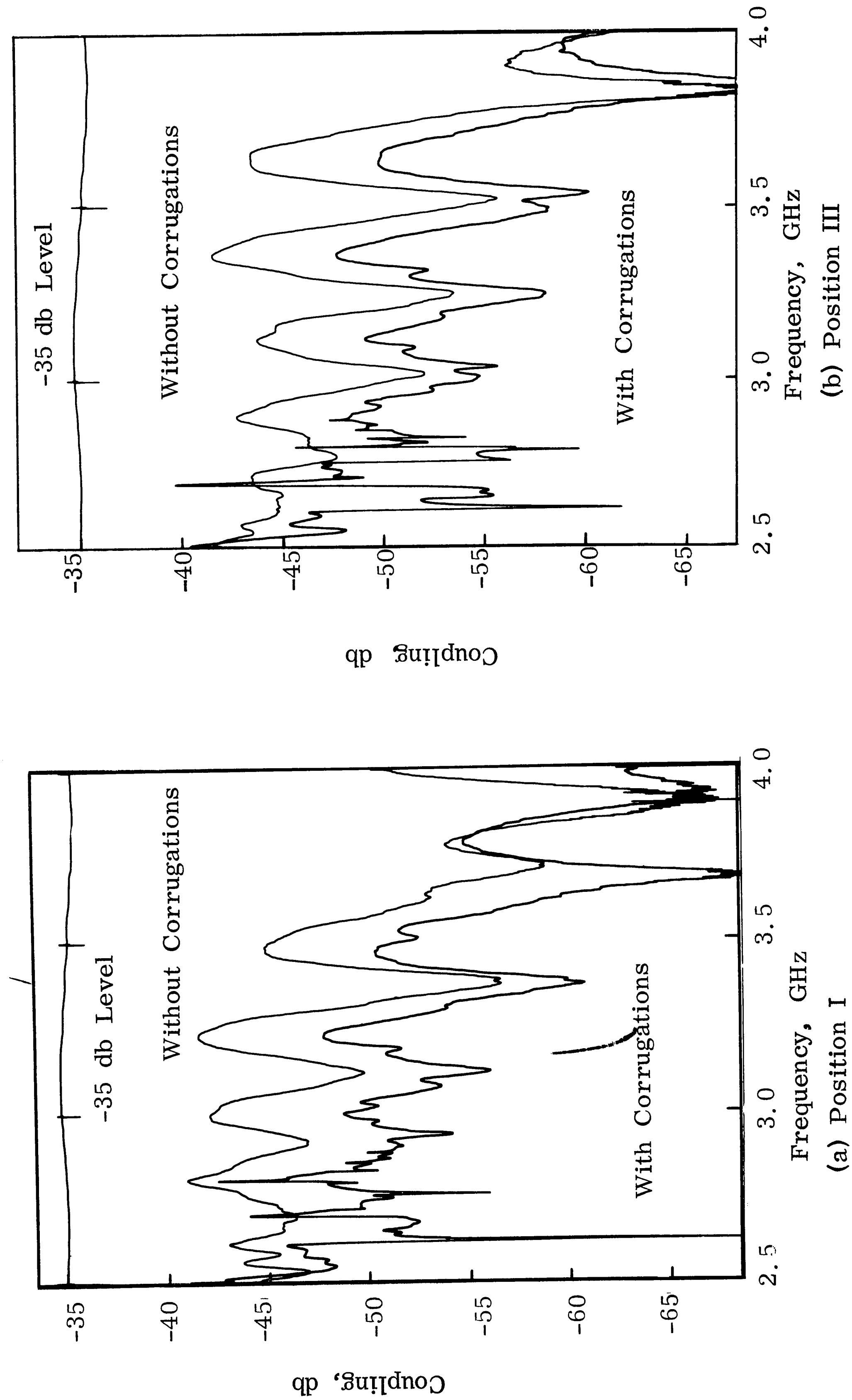

FIG. 2-8: COUPLING VS FREQUENCY FOR TWO ARCHIMEDEAN SPIRALS SPACED 22.8 CM.

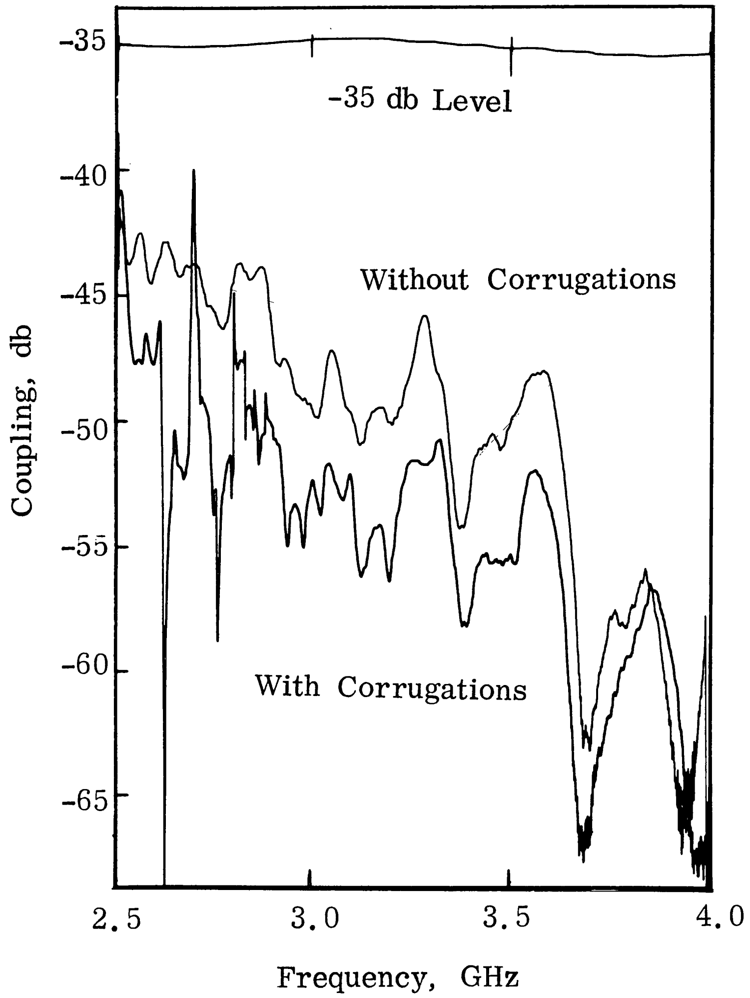

(c) Position II

FIG. 2-8: CONTINUED.

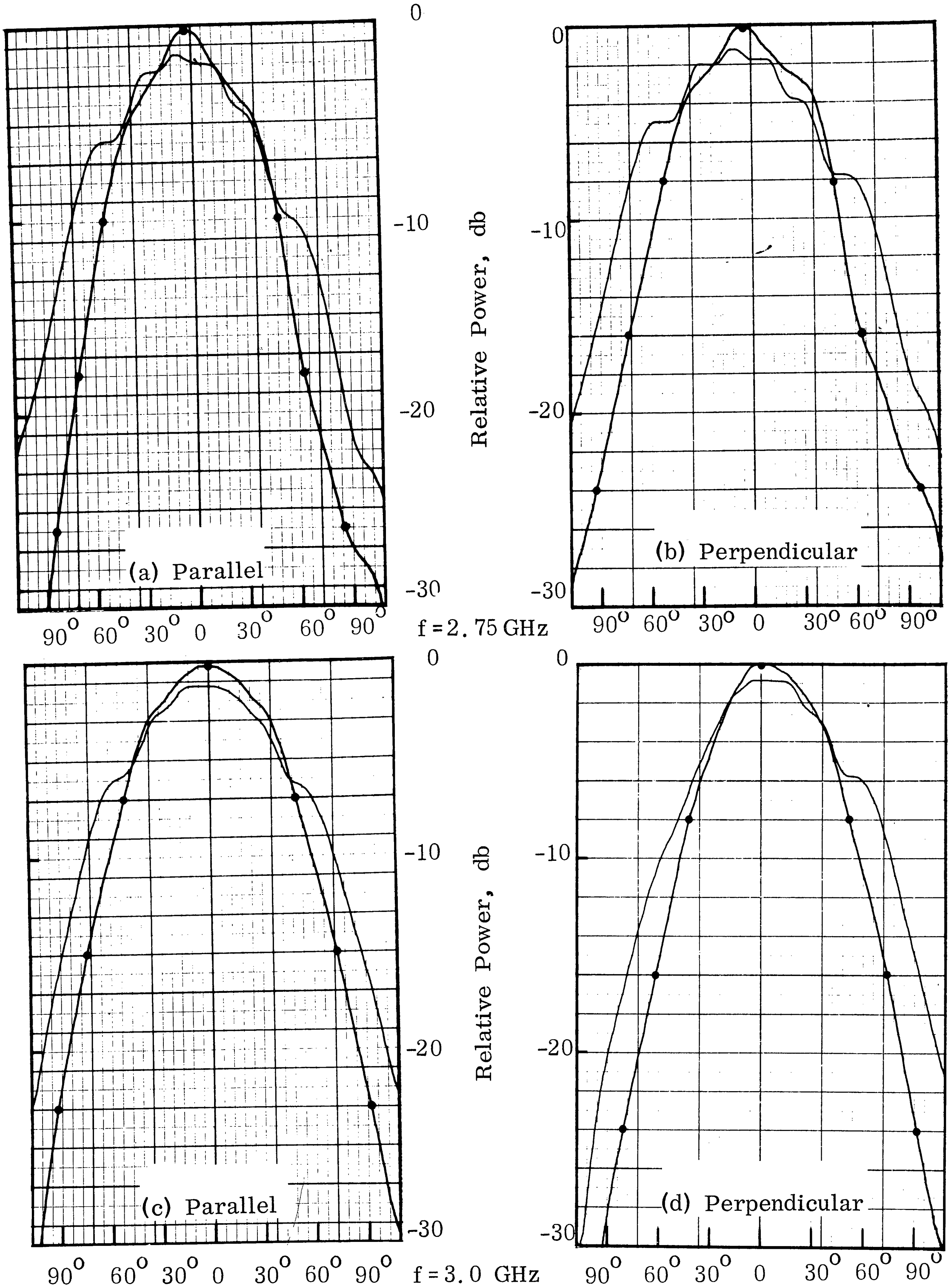

FIG. 2-9: RADIATION PATTERNS OF AN ARCHIMEDEAN SPIRAL IN A 2 FT. BY 3 FT. METAL GROUND PLANE FOR TWO NORMAL LINEAR POLARIZATIONS. (—) Flat Plane; (—o—) With Corrugations.

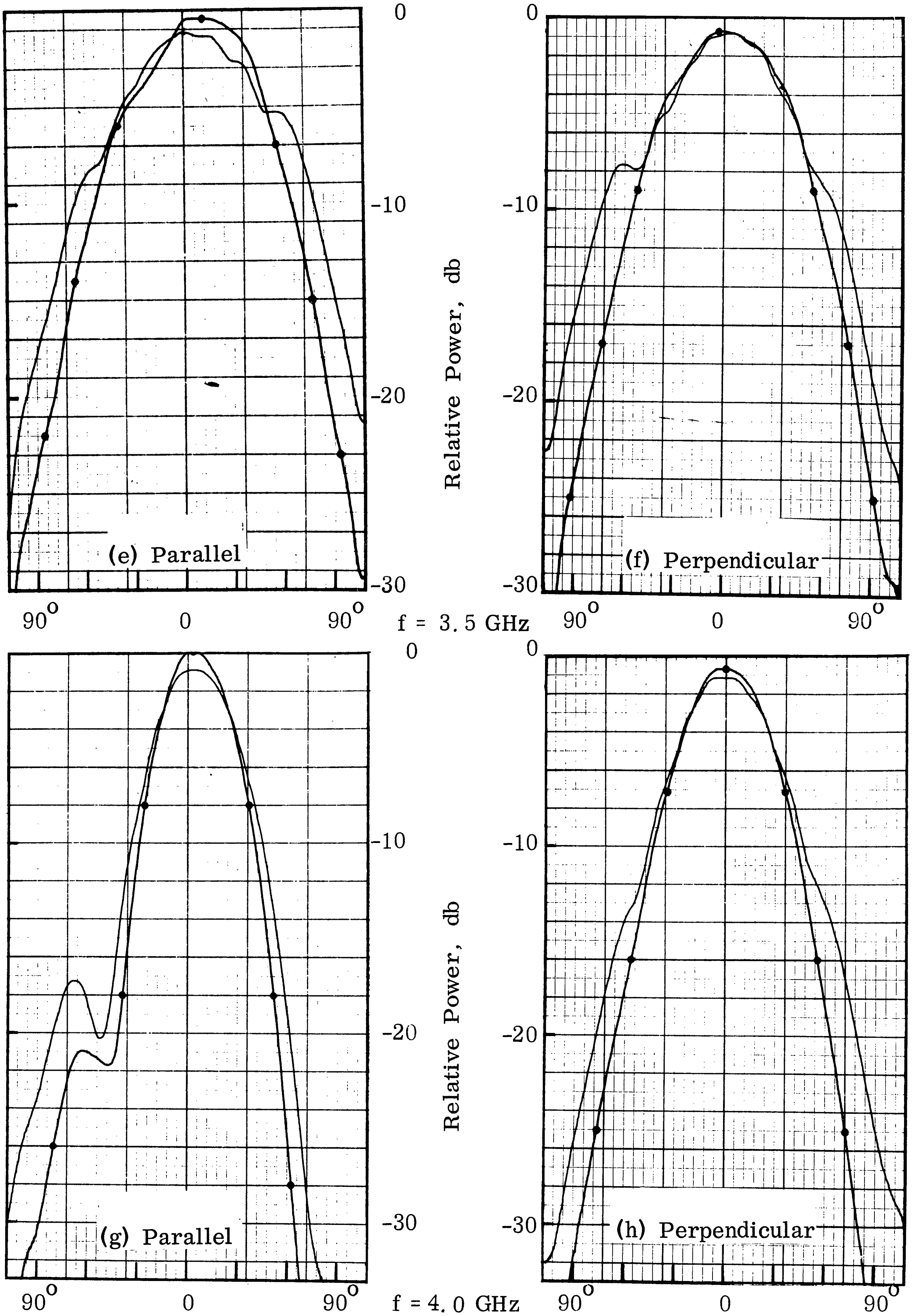

FIG. 2-9: CONTINUED

TABLE II

Spiral Standing Wave Ratio

Frequency, GHz	2.75	3.00	3.25	3.50	3.75	4.00
Flat Ground Plane	1.45	1.33	1.26	1.90	1.79	1.75
With Corrugations	1.60	1.42	1.47	1.31	1.40	1.37

2.2 Coupling Under Dielectric Layers

Experimental studies are being made to investigate the coupling of two X-band slot antennas covered by a dielectric sheet. The antennas being used in these studies are two waveguide-fed slots mounted in a 12 ft. by 12 ft. aluminum ground plane. The antennas are oriented for the strong or E-plane coupling case, and the separation is 11.4 cm. All measurements use a swept-frequency technique from 8 GHz to 12.4 GHz.

The material used in early experiments was California Sugar Pine. This material has $\epsilon_r = 1.7$ and a dissipation factor D = 0.010. These are approximate tabulated values and not measured data. This material was used only because it was readily available, cheap, and easy to utilize. Because of the non-isotopic properties of the wood grain and the relatively high loss, this material was abandoned as soon as other more desirable materials became available.

One such material is polystyrene, which has $\epsilon_r = 2.5$ and a dissipation factor D = 0.0004. Sheets were obtained in 20 inch by 40 inch size with three thicknesses, 1/8 inch, 1/4 inch, and 1/2 inch. Data are presented for the coupling with each of these sheets in Figs. 2-10, 2-11, and 2-12. Each figure shows the direct coupled level and the coupling of two plain slots, along with two curves for the coupling with the polystyrene sheet. The dotted polystyrene curve corresponds to the 40 inch dimension in the H-plane. Note that in some cases the coupling level with the polystyrene sheets is 4 to 5 db higher than the plain slot case, but in one case there is some actual decoupling over part of the band. It is this decoupled case that is of interest, and it will be studied in more detail.

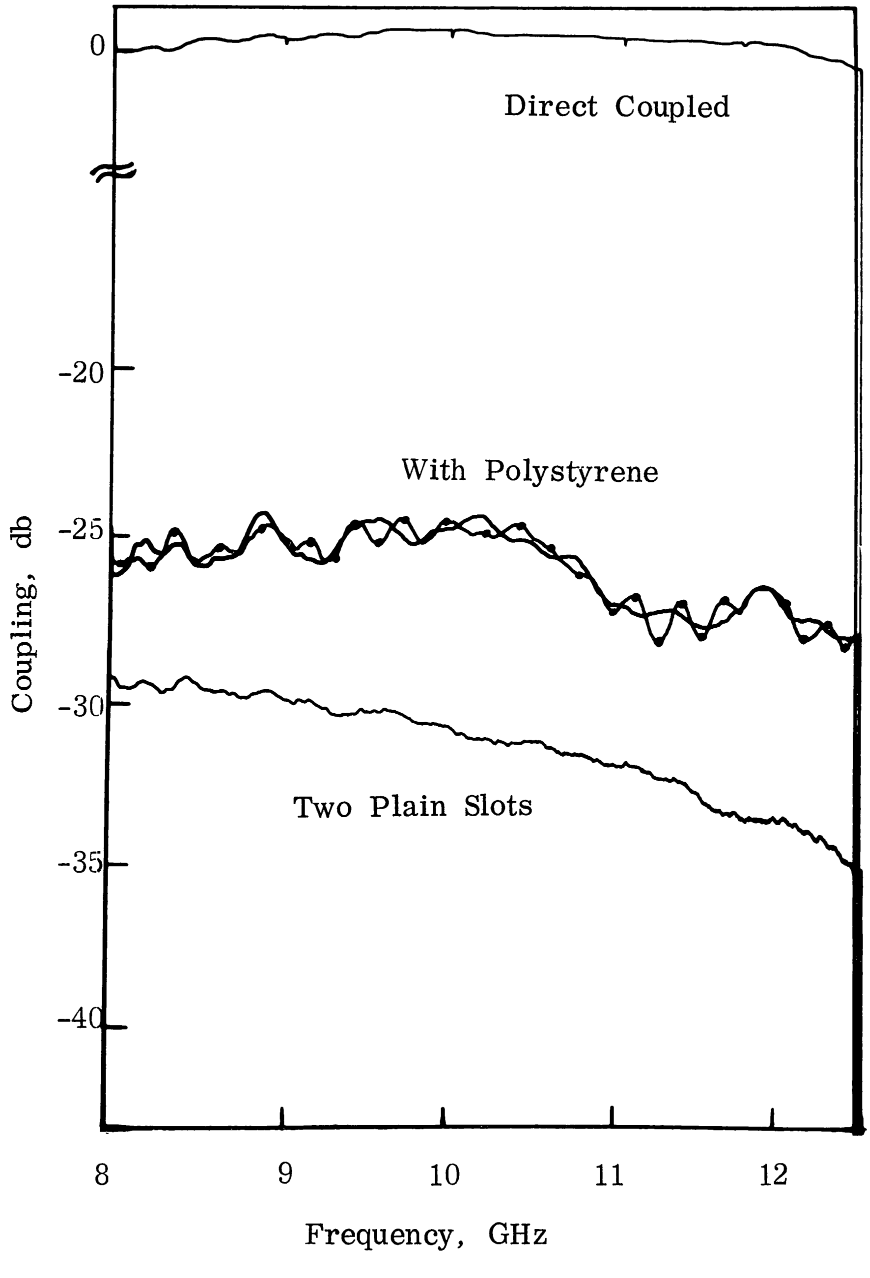

FIG. 2-10: SLOT COUPLING WITH 40 INCH BY 20 INCH BY 1/8 INCH POLYSTYRENE SHEET.

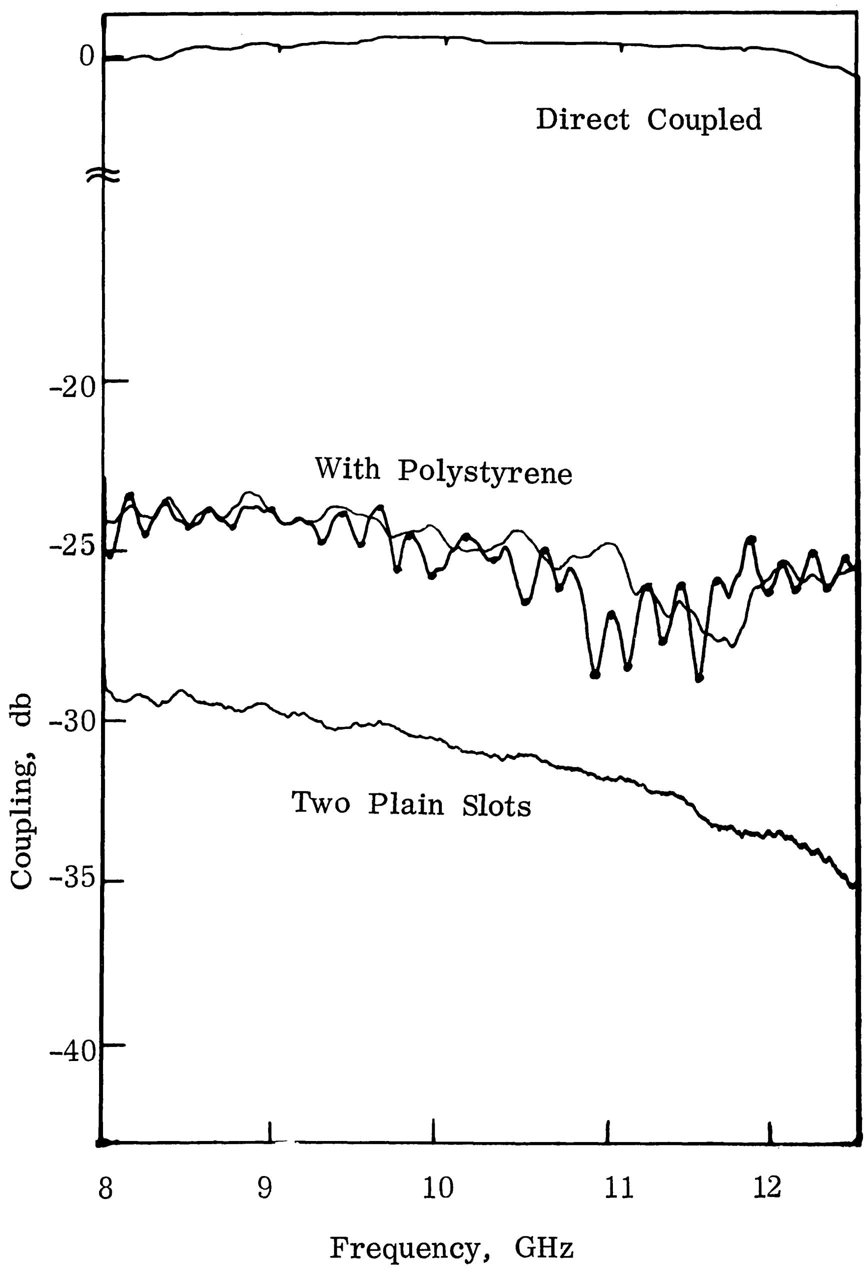

FIG. 2-11: SLOT COUPLING WITH 40 INCH BY 20 INCH BY 1/4 INCH POLYSTYRENE SHEET.

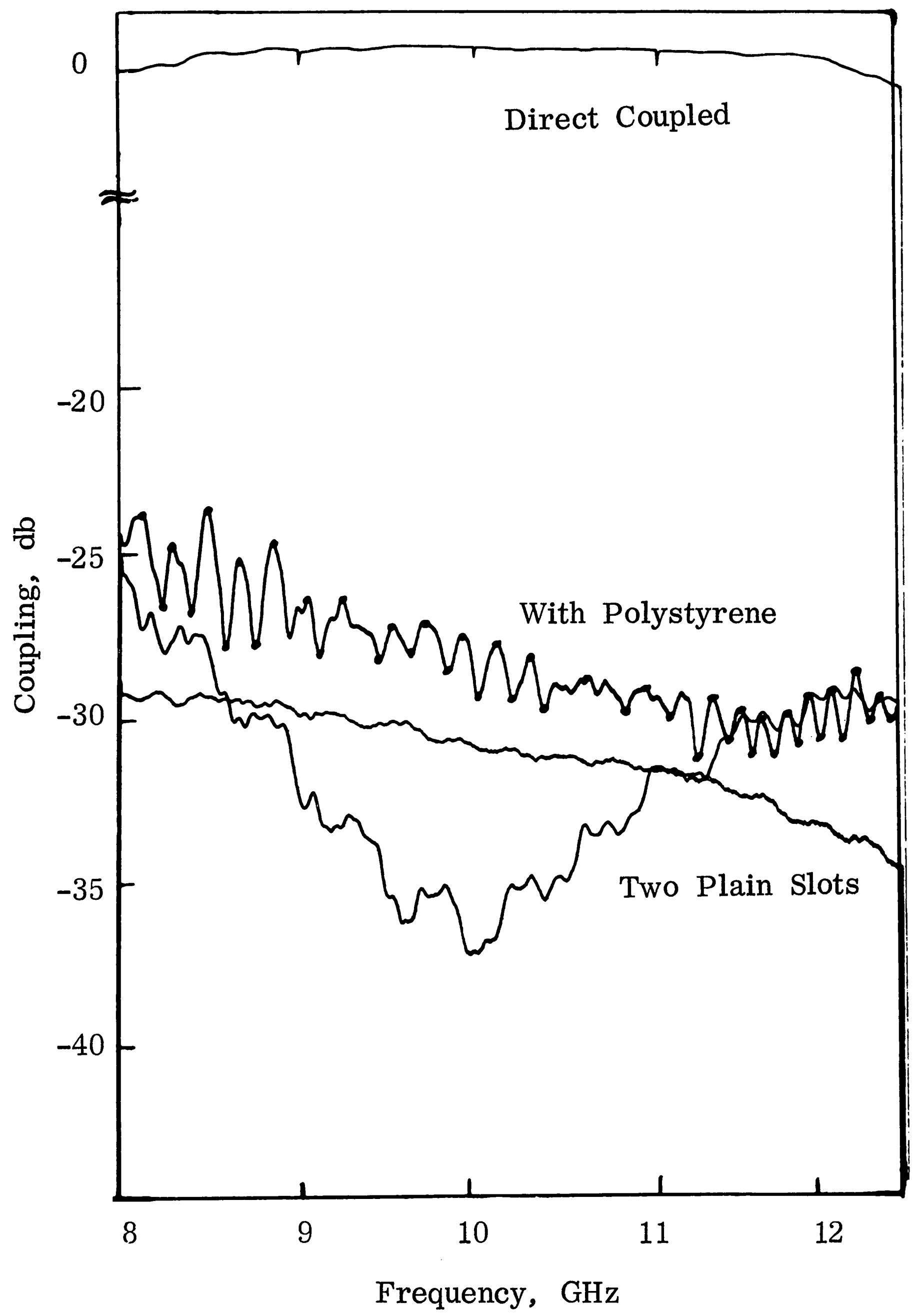

FIG. 2-12: SLOT COUPLING WITH 40 INCH BY 20 INCH BY 1/2 INCH POLYSTYRENE SHEET.

Notice that the coupling curves with the polystyrene sheets have periodic fluctuations. These fluctuations seem to be due to reflections from the edges of the sheets in the E-plane direction. To see this, the range of the scatterer may be calculated using the formula:

$$R = 1/2\left[\frac{nv}{\Delta f} + R_o\right] \quad \text{for } R \gg R_o \tag{2-4}$$

Where: R is the range of the scatterer.

n is the number of cycles.

Δf is the frequency sweep.

R_o is the distance between antennas.

v is the velocity of propagation.

Counting the cycles in Fig. 2-11, (the dotted curve), one finds n = 20. For the other values: $R_o = 4.5$ inches, $\Delta f = 4.2$ GHz, and $v = c/\sqrt{2.5}$.

Making the calculation, one finds R = 20 inches. Note that this is exactly the distance from the E-plane edge of the polystyrene sheet to the center of the two antennas.

2.3 Theoretical Analysis of Slots in a Ground Plane

Previously, analysis has been presented which shows a relatively simplified way of computing coupling between two rectangular slots when the slots are in the far field region. More recently, additional theoretical investigation has been resumed on the calculation of coupling between two rectangular slots mounted in an infinite ground plane. These rectangular slots are oriented so that the E-planes are parallel, or in other words for the strong coupling situation. The analysis includes the cases for the slots being filled with either dielectric or ferrite material. Also this analysis will endeavor to predict the near field coupling as well as the far field coupling situations.

An experimental arrangement is being prepared to measure the effect on coupling between the two rectangular slots in the ground plane as a function of the loading material in the slots. Each slot is backed by a short cavity which in turn is fed by means of a coaxial cable.

It is expected that measurements will indicate the dependence of the coupling between the slots on materials having various electrical parameters. The dependence of the illumination of the transmitting slot on the frequency of operation as compared to the cutoff will be carefully studied. For the present, experimental work has been planned for the X-band range of frequency.

The main accomplishment during this report period has been a substantial start on improved formulation of the coupling situation. Some of the experiments have been designed but measurements have yet to be initiated.

2.4 Current Distribution on a Rectangular Spiral Antenna.

The current distribution along the windings of a VHF-UHF two-arm rectangular spiral has been measured. When the antenna is excited in push-pull as a transmitting antenna, the current is found to be of the form of an outgoing traveling wave. The phase constant along the winding is very close to the free space phase constant although the derivative tends to be high around the corners. Fig. 2-13 shows the result as measured at f = 400 MHz. It is more difficult to associate a single attenuation constant with the current going down the windings as can be seen from the figure. The most abrupt change in the magnitude usually occurs around the corners. When the antenna is considered as a scatterer, however, the current on the windings is seen to depend very much upon the form of the incident wave. Two questions of interest arise at this point. One is whether traveling waves exist on the windings as in the case when the spiral is used as a transmitting antenna. Both linearly and circularly polarized waves have been used as the incident wave to this end and no traveling

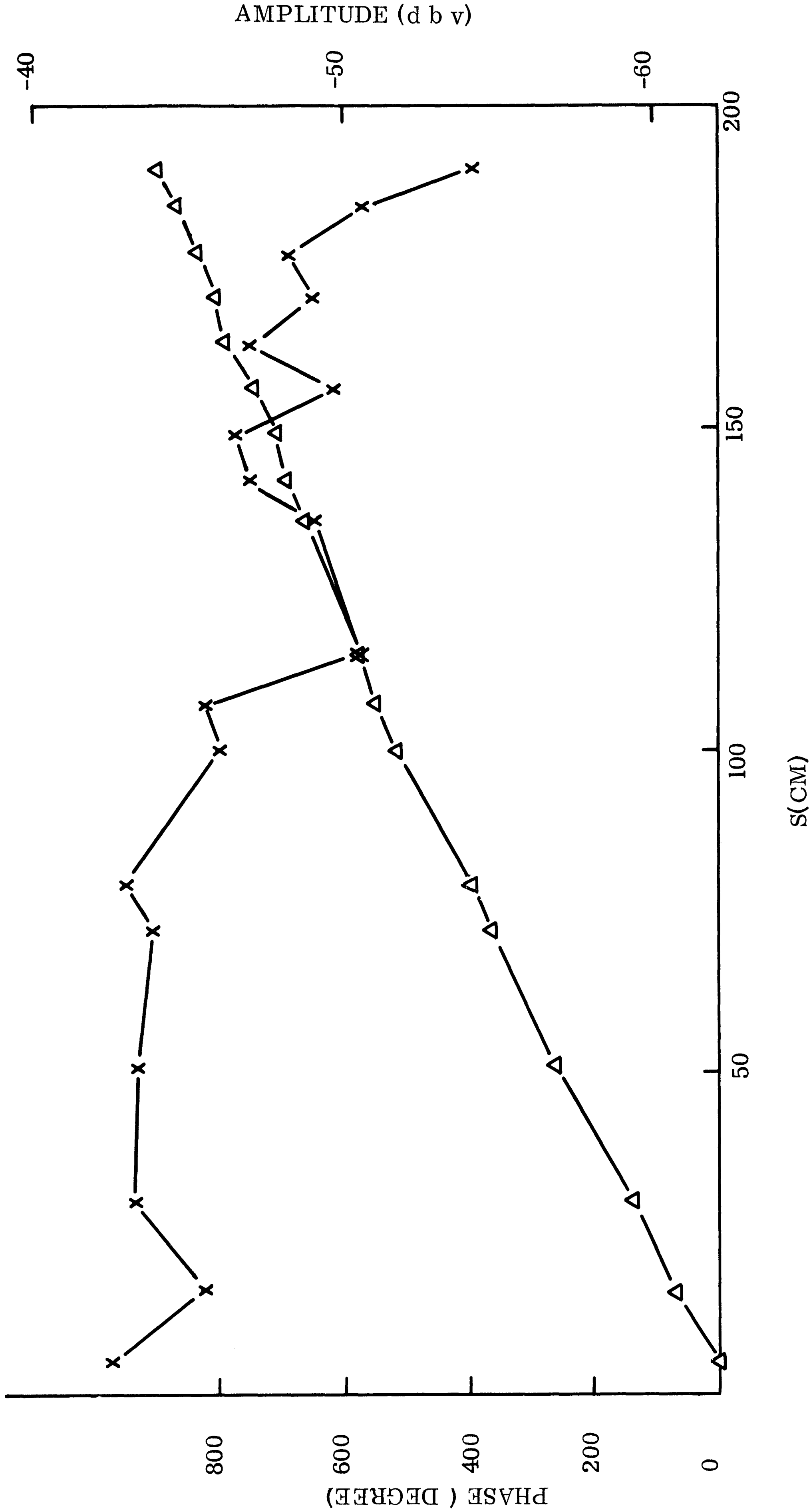

FIGURE 2-13 AMPLITUDE AND PHASE OF THE CURRENT EXCITED ON ONE ARM OF THE RECTANGULAR SPIRAL. f=400MHz(x)AMPLITUDE (△) PHASE:

waves have been observed so far. The other question is what happens when the antenna is illuminated with an infinite plane wave. A spherical wave was produced by another antenna to approximate a plane wave. The magnitude and phase of this spherical wave over a large portion of the rectangular spiral has relatively small variations. The magnetic field transverse to the windings of the spiral was measured along an axis X-X of the spiral as shown in Fig. 2-14. Afterwards, the scatterer was removed and the field measured again. A typical result is shown in Fig. 2-15. The scatterer spiral is seen to have only second order effects on the total field since both the magnitude and the phase of the total field do not exhibit any drastic change in the presence of the spiral scatterer. It should be mentioned here that the spiral used is not backed by a metal cavity. In this particular case, the form of the current excited on the windings of the spiral and the effect of the terminal conditions of the spiral cannot be seen from the figure. This is because the incident field rather than the scattered field largely accounts for the total field measured.

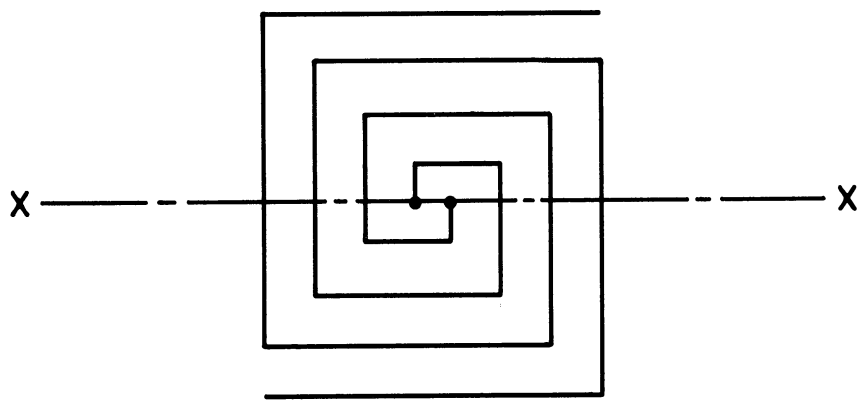

$H_{transvere} = H_x$

FIG. 2-14 MEASUREMENT OF THE TRANSVERSE COMPONENT OF H-FIELD ALONG AN AXIS X-X ON THE SPIRAL SURFACE.

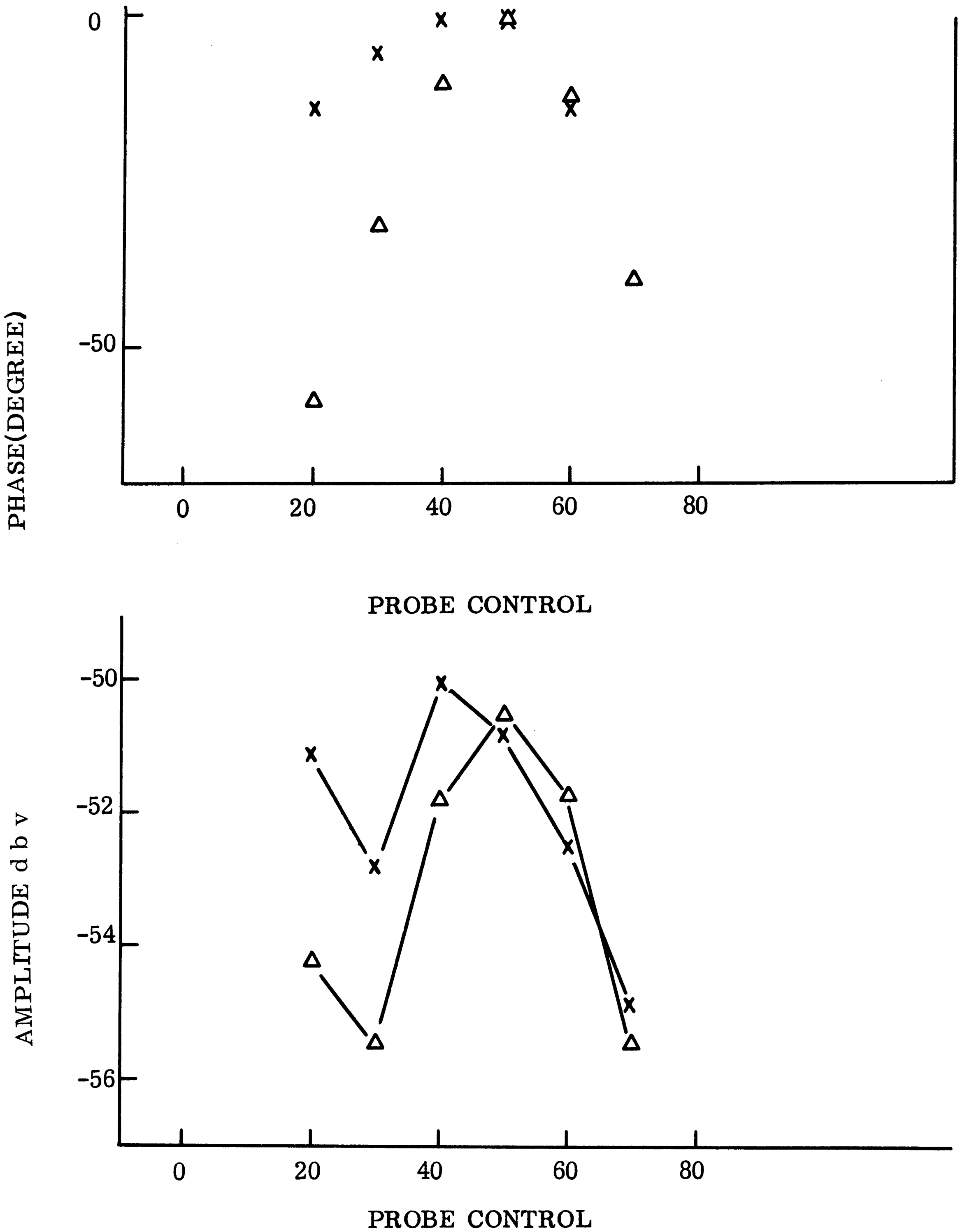

FIG. 2-15 AMPLITUDE AND PHASE OF H FIELD WITH AND WITHOUT THE SPIRAL SCATTERER IN PLACE.
(Δ) WITH SPIRAL (X) WITHOUT SPIRAL.

III

CONCLUSIONS

The results recorded on corrugations continue to be very satisfactory for any range of frequencies where there is sufficient room for adequately designed set of corrugations. This appears to be one of the most useful means of achieving decoupling. Experimental results for this method have been obtained at S-band as well as X-band. Furthermore, the evidence presented shows that it is appropriate to have a set of corrugations which will also operate satisfactorily at 3 times the design frequency. This means that a set of corrugations can be very helpful both for decoupling the fundamental but also the third harmonic from a transmitting antenna. Corrugations have proved useful in reducing coupling between Archimedian spirals as well as rectangular slots.

The study of dielectric cover plates over slot antennas has not been completed. However, the results indicated to date, show that this is a relatively complicated problem. As yet, a systematic method of predicting the influence of such plates has not been achieved. However, the results are consistent with fundamental concepts as applied to the physical situations covered.

The advanced analysis, which has just begun on two rectangular slot antennas has not been sufficiently completed so that conclusions may be drawn. However, it appears that sufficient accuracy can be obtained using approximations and computer methods to enable and adequate prediction.

IV

FUTURE EFFORT

It is expected that sufficient effort will be placed upon corrugations to indicate more fully, the extent of applicability of this means of decoupling. The study of dielectric cover plates and the influence on coupling and decoupling has only been initiated as far as the experimental part of the program. During the next period, more experimental work and some applicable analysis will be performed. Analytical results will be compared with the experimental data.

During the next period, a major effort will be made to advance the analysis on parallel slots at least to a point where some predictions of behavior can be made. It is difficult to predict the success of this analysis by the use of appropriate approximation and computer facilities, it is hoped that this analysis will give further insight on the nearfield coupling situation.

ACKNOWLEDGEMENT

Mr. D.R. Brundage of The University of Michigan, Institute of Science and Technology performed some of the experimental work reported here.

REFERENCES

Lyon, J.A.M. et al (May 1966), "Electromagnetic Coupling Reduction Techniques," The University of Michigan, Radiation Laboratory, Report 7692-2-Q, pg. 24.

Watkins, D.A. (1958), Topics in Electromagnetic Theory, J. Wiley and Sons, New York, pg. 18.

DISTRIBUTION LIST AF 33(615)-3371 Proj. 07692

Destination	Number of Copies
Aerospace Corporation Mr. Robert C. Hansen 2400 E. El Segundo Blvd. Los Angeles, Calif. 90045	1
Andrew Alfred Consulting Engineers Librarian - Antenna Section 299 Atlantic Avenue Boston, Mass. 02110	1
Bell Telephone Laboratories, Inc. Room 2A165 - Technical Reports Librarian Whippany, New Jersey 07961	1
Bendix Research Laboratories Technical Reports Librarian 20800 10 1/2 Mile Road Southfield, Michigan 48076	1
Boeing Aerospace Division Technical Library - Antenna and Radomes P.O. Box 3707 Seattle, Washington 98124	1
Collins Radio Corporation Dr. Robert L. Carrel Antenna Section Dallas, Texas 75207	1
Douglas Aircraft Company MSSD Technical Library - Antennas 3000 Ocean Park Blvd. Santa Monica, Calif. 90406	1
General Dynamics/Fort Worth Technical Library - Antennas P.O. Box 748 Fort Worth, Texas 76101	1
General Electric Electronics Laboratory Technical Library Electronics Park Syracuse, New York 13201	1
Hughes Aircraft Company Technical Library - Antennas Centinela and Teale Streets Culver City, Calif. 90232	1
ITT Federal Laboratories Technical Library - Antennas 500 Washington Ave. Nutley, New Jersey 07710	1

Ling-Temco-Vought
Military Electronics Division
Librarian - Antennas
1200 Jupiter Street
Garland, Texas 75222 1

RCA Missile and Service Radar Division
Manager, Antenna Engineering Skill Center
Marne Highway
Moorestown, N.J. 08057 1

Raytheon Space and Information Systems Division
Attn: Antenna Group
Box 1542
Goleta, California 93017 1

Lockheed Electronic and Armaments Systems
Technical Library
P.O. Box 551
Burbank, California 91503 1

Martin/Denver Antenna Laboratory
Mail Nr. T-0453
P.O. Box 179
Denver, Colorado 80201 1

McDonnell Aircraft Corporation
Technical Library - Antennas
Box 516
St. Louis, Mo. 63166 1

Motorola Western Military Electronics Div.
Technical Librarian
8201 E. McDowell
Scottsdale, Arizona 85252 1

North American Aviation, Inc.
Technical Library - Engineering Dept.
4300 E. Fifth Avenue
Columbus, Ohio 43216 1

Space Technology Laboratory
Research Library
One Space Park
Redondo Beach, California 90278 1

Stanford Research Institute
Librarian - Antenna Laboratory
Ravenswood Street
Menlo Park, California 94025 1

Sylvania Electronic Systems Division Librarian - Antennas and Microwaves 40 Sylvan Street Waltham, Mass. 02154	1
Westinghouse Aerospace Division P. O. Box 746 Baltimore, Md. 21203	1
Air Force Avionics Laboratory AVWE-3 Wright-Patterson AFB, Ohio 45433	6
Systems Engineering Group Mr. Mulligan SEAFM Wright-Patterson AFB, Ohio 45433	1
Systems Engineering Group SEPIE Wright-Patterson AFB, Ohio 45433	1
Air Force Cambridge Research Laboratories C. J. Sletten CRD L. G. Hanscom Field Bedford, Mass 01731	1
AFETRL - Technical Library Patrick AFB, Florida 32925	1
AFMDC - Technical Library Holloman AFB, New Mexico 88330	1
RADC EMTLT-1 Griffiss AFB, New York 13442	1
ESD - ESRRE L. G. Hanscom Field Bedford, Mass. 01731	1
RTD RTTC Bolling AFB, Washington, D. C. 20332	1
USAF - Major Jaffers : AFRST Washington, D. C. 20330	1
Office of Aerospace Research Building T-3 Washington, D. C. 20333	1
RADC EMCRV Griffiss AFB, New York 13442	1

Aeronautical Systems Division - AVS Wright-Patterson AFB, Ohio 45433	1
Aeronautical Systems Division - ASZFT Wright-Patterson AFB, Ohio 45433	1
Aeronautical Systems Division - ASZIE Wright-Patterson AFB, Ohio 45433	1
Aeronautical Systems Division - ASZW Wright-Patterson AFB, Ohio 45433	1
Aeronautical Systems Division - ASTFP Wright-Patterson AFB, Ohio 45433	1
Systems Engineering Group - SEACR Wright-Patterson AFB, Ohio 45433	1
AFIT Wright-Patterson AFB, Ohio 45433	1
Electromagnetic Compatibility Analysis Center Code ACG U. S. Navy Marine Engineering Laboratory Annapolis, Md. 21402	1
Electromagnetic Compatibility Analysis Center Code ACZ U. S. Navy Marine Engineering Laboratory Annapolis, Md. 21402	1
Electromagnetic Compatibility Analysis Center Code ACO U. S. Navy Marine Engineering Laboratory Annapolis, Md. 21402	1
RADC - EMATA Griffiss AFB, New York 13442	1
RADC EMIAD Mr. R. F. Davis Griffiss AFB, New York 13442	1
AFSC - SCSE Andrews AFB, Washington D C 20330	1
USAF - Lt. Col. B. Lieber AFRDRE Washington, D. C. 20330	1

Hq, USAF, AFISAI Air Battle Analysis Center Deputy Director, Plans for War Plans Directorate of Plans SCS/P and O Washington, D. C. 20330	1
RTD RTTR Bolling AFB, Washington, D.C. 20332	1
Office, Assist. Sec'y Defense (R and D) Room 3E1065, Technical Library - Pentagon Washington, D.C. 20330	1
USAFSS ESD: ESG. Mr. A. Martinez San Antonio, Texas 78241	1
U.S. Army Electronics Command SIGRA/NAI Fort Monmouth, N. J. 07703	1
U.S. Army White Sands Missile Range Technical Library RR-312 White Sands, New Mexico 88002	1
Harry Diamond Laboratories - Code 240 Connecticut Ave. and Van Ness Street, NW Washington, D.C. 20433	1
NASA Goddard Space Flight Center Antenna Branch - Code 525 Greenbelt, Md. 20771	1
U.S. Naval Research Laboratory Code 5200 Washington, D.C. 20390	1
U.S. Naval Test Center WSST-54, Antenna Section Patuxent River, Md. 20910	1
Air University Library 3T-AUL-59-30 Maxwell AFB, Alabama 36112	1
RTD RTGS Bolling, AFB, Washington, D.C. 20332	1
FTD TDEE Wright-Patterson AFB, Ohio 45433	1
V. DeSanti, Chief, Exchange Section DCS Scientific/Technical Information Facility Box 7500 Bethesda, Md.	1

Cornell Aeronautical Laboratory Research Library Buffalo, New York 14221	1
GIT - Engineering Experiment Station Technical Library - Electronics Division Atlanta, Ga. 30313	1
Johns Hopkins University Carlyle Barton Laboratory Charles and 34th Street Baltimore, Md. 22218	1
MIT-Lincoln Laboratory Document Room - E. Brans Box 73 Lexington, Mass 02173	1
Ohio State University Research Foundation Technical Library - Antenna Laboratory 2024 Neil Avenue Columbus, Ohio 43210	1
PIB - Microwave Research Institute A. A. Oliner 55 Johnson Street Brooklyn, N. Y. 11201	1
Stanford Electronics Laboratory Librarian - Antenna Laboratory Stanford, California 94025	1
Syracuse University Dr. Jose Perihi - EE Department Syracuse, N. Y. 13210	1
University of Southern California W. V. Trusch - EE Department University Park Los Angeles, California 90007	1
Defense Documentation Center Cameron Station Alexandria, Va. 22314	20
	97

UNCLASSIFIED

Security Classification

DOCUMENT CONTROL DATA - R & D

(Security classification of title, body of abstract and indexing annotation must be entered when the overall report is classified)

1. ORIGINATING ACTIVITY *(Corporate author)* The University of Michigan Radiation Laboratory, Dept. of Electrical Engineering, 201 Catherine Street, Ann Arbor, Michigan 48108	2a. REPORT SECURITY CLASSIFICATION Unclassified
	2b. GROUP

3. REPORT TITLE

ELECTROMAGNETIC COUPLING REDUCTION TECHNIQUES

4. DESCRIPTIVE NOTES *(Type of report and inclusive dates)*

Eighth Quarterly Report 15 August through 14 November 1967

5. AUTHOR(S) *(First name, middle initial, last name)*

John A. M. Lyon, Constantine J. Digenis, William W. Parker, Alan G. Cha and Medhat A. H. Ibrahim.

6. REPORT DATE	7a. TOTAL NO. OF PAGES	7b. NO. OF REFS
December 1967	31	2

8a. CONTRACT OR GRANT NO. AF 33(615)-3371	9a. ORIGINATOR'S REPORT NUMBER(S) 7692-8-Q
b. PROJECT NO. 4357	
c. Task 435709	9b. OTHER REPORT NO(S) *(Any other numbers that may be assigned this report)*
d.	

10. DISTRIBUTION STATEMENT

Available from DDC. Subject to special export controls. Transmittal to foreign governments or nationals may be made only with prior approval from AFAL, AVPT, Wright-Patterson AFB, Ohio 45433.

11. SUPPLEMENTARY NOTES	12. SPONSORING MILITARY ACTIVITY
	Air Force Avionics Laboratory, AVWE United States Air Force, AFSC Wright-Patterson AFB, Ohio 45433

13. ABSTRACT

In this report further studies on some previously described decoupling methods are presented. Slot decoupling has been examined at a lower range of frequencies (S-band). The behavior of corrugations at three times the design frequency has also been studied. The use of circumferential corrugations as a decoupling means was extended to circular Archimedean spiral antennas. Studies initiated in this report period included the coupling of two X-band slot antennas covered by a dielectric sheet. It has been found that under some conditions the presence of the sheet results in decoupling, whereas in other cases increased coupling results.

DD FORM 1 NOV 65 1473

Security Classification

14. KEY WORDS	LINK A		LINK B		LINK C	
	ROLE	WT	ROLE	WT	ROLE	WT
ANTENNA COUPLING						
ANTENNA DECOUPLING						
ANTENNA ISOLATION						
ANTENNA INTERFERENCE						